JULY 1982 LRP 207/82

EFFECTS OF FINITE ION CYCLOTRON FREQUENCY ON THE ABSORPTION OF MAGNETOHYDRODYNAMIC WAVES AT THE SPATIAL ALFVEN RESONANCE

K. Appert and J. Vaclavik

EFFECTS OF FINITE ION CYCLOTRON FREQUENCY ON THE ABSORPTION OF MAGNETOHYDRODYNAMIC WAVES AT THE SPATIAL ALFVEN RESONANCE

K. Appert and J. Vaclavik

Centre de Recherches en Physique des Plasmas
Association Euratom - Confédération Suisse
Ecole Polytechnique Fédérale de Lausanne
21, Av. des Bains, CH-1007 Lausanne, Switzerland

ABSTRACT

The absorption of magnetoacoustic modes at the spatial Alfvén resonance of Tokamak plasmas is investigated within the context of an ideal MHD model which includes finite ω/ω_{ci} effects. It is found that these effects can dramatically modify the pure MHD picture of the resonant absorption and the spectrum of global eigenmodes of the Alfvén wave. Implications for the interpretation of recent experimental results are discussed.

1. INTRODUCTION

The absorption of r.f. fields at the Alfvén resonance layer in nonuniform plasmas is one of the principal features of Alfvén wave heating. For Tokamaks two schemes of the resonant absorption have been considered: 1) the excitation of the first radial eigenmode of the fast magnetoacoustic wave (so called "surface mode") (GROSSMANN and TATARONIS, 1973; HASEGAWA and CHEN, 1974), 2) the excitation of higher radial eigenmodes of the fast magnetoacoustic wave (so called "cavity modes") (STIX, 1976). In our previous work (BALET et al., 1982) we tried to provide a unified picture of these schemes from an MHD viewpoint. It was found that the first scheme is much more efficient, as far as the deposition of the wave energy in the centre of the plasma is concerned, than the second one. Of course, these results were obtained in the limit $\omega/\omega_{ci} \to 0$, where ω and ω_{ci} are the excitation and ion cyclotron frequencies, respectively. However, for parameters typical of present day Tokamaks the ω/ω_{ci} ratio appears not to be very small. Thus, there is an incentive for a systematic study of the effects of a finite ω/ω_{ci} ratio on the resonant absorption of the magnetoacoustic modes. This problem is addressed in the present paper. Previous treatments of the problem were confined either to a slab geometry, uniform magnetic field and linear density profile (KARNEY et al., 1979; STIX, 1980) or to some specific examples of machines and excitations (ROSS et al., 1982).

The paper is structured as follows. In Section 2 we derive the basic equations of our model and present some qualitative considerations. The equations are solved numerically and the results are presented in Section 3. Finally, we draw the main conclusions in Section 4.

2. BASIC EQUATIONS

We consider small-amplitude perturbations with frequencies $\omega \lesssim \omega_{ci}$ in a cold current-carrying plasma. The plasma motion can then be described by the linearized equation of momentum transfer

$$\rho \frac{\partial \vec{v}}{\partial t} = \frac{1}{c}\left(\vec{j} \times \vec{B}_0 + \vec{j}_0 \times \vec{B}\right) \tag{1}$$

and the linearized Ohm law which includes the Hall term

$$\vec{E} + \frac{1}{c}\left(\vec{v} \times \vec{B}_0\right) = \frac{m_i}{ec\rho}\left(\vec{j} \times \vec{B}_0 + \vec{j}_0 \times \vec{B}\right). \tag{2}$$

Here $\vec{v}$ is the plasma velocity, $\vec{j}$ and $\vec{j}_0$ are the perturbation and equilibrium current densities, $\vec{B}$ and $\vec{B}_0$ are the perturbation and equilibrium magnetic fields, ρ is the equilibrium mass density, c is the velocity of light, $\vec{E}$ is the electric field, e is the electron charge and m_i is the ion mass.

We adopt a cylindrical geometry and assume that the equilibrium quantities are functions of radius r only. We may then take the time and space dependence of the perturbation quantities as $\exp\{i[kz+m\Theta - (\omega+i\nu)t]\}$, where k and m are the axial and azimuthal wavenumbers, and $\nu \to 0_+$. To proceed further we introduce a local coordinate system with $\hat{r}$, $\hat{e}_\perp = \hat{e}_\parallel \times \hat{r}$, $\hat{e}_\parallel = \vec{B}_0/B_0$ and assume B_{0z} = const. and $|B_{0\theta}/B_{0z}| \ll 1$. On combining equations (1) and (2) with the Faraday law we can determine a relation between $\vec{j}$ and $\vec{E}$, and hence obtain the expression for the plasma dielectric tensor $\overleftrightarrow{\varepsilon}$. Up to the first order in $B_{0\theta}/B_{0z}$ and for $c/c_A \gg 1$ we find

$$\varepsilon_{rr} = \varepsilon_{\perp\perp} = \left(\frac{c}{c_A}\right)^2 \frac{1}{1-(\omega/\omega_{ci})^2} \quad , \tag{3}$$

$$\varepsilon_{r\perp} = -\varepsilon_{\perp r} = i\left[\left(\frac{c}{c_A}\right)^2 \frac{\omega/\omega_{ci}}{1-(\omega/\omega_{ci})^2} - \left(\frac{c}{\omega}\right)^2 \frac{k_\parallel}{r} \frac{d}{dr}\left(\frac{rB_{0\theta}}{B_{0z}}\right)\right] , \tag{4}$$

where c_A is the Alfvén speed and $k_\parallel B_0 = kB_{0z} + (m/r)B_{0\theta}$. The other components of $\overleftrightarrow{\varepsilon}$ are not needed since the Ohm law implies $E_\parallel = 0$.

On substituting the expressions (3) and (4) into the Maxwell equations expanded up to the first order in $B_{0\theta}/B_{0z}$ we obtain two coupled first-order equations for the quantities $E_\perp$ and $B_\parallel$

$$A\frac{1}{r}\frac{d}{dr}(rE_\perp) = Gk_\perp E_\perp + \frac{i\omega}{c}(A-k_\perp^2)B_\parallel \quad , \tag{5}$$

$$A\frac{dB_\parallel}{dr} = \frac{c}{i\omega}\left(G^2-A^2\right)E_\perp - Gk_\perp B_\parallel \quad , \tag{6}$$

where

$$A = \left(\frac{\omega}{c_A}\right)^2 \frac{1}{1-(\omega/\omega_{ci})^2} - k_\parallel^2 \quad , \tag{7}$$

$$G = \left(\frac{\omega}{c_A}\right)^2 \frac{\omega/\omega_{ci}}{1-(\omega/\omega_{ci})^2} - \frac{2B_{o\theta}}{rB_{oz}} k_\parallel \tag{8}$$

and $k_\perp B_o = (m/r)B_{oz} - kB_{o\theta}$.

Equations (5) and (6) are the basic equations of our model. We note that they have the same structure as the equations derived recently for the case $\omega/\omega_{ci} = 0$ (APPERT et al., 1982 a and b). The finite frequency corrections cause only a modification of the coefficients A and G in the latter. The first term of A is divided by the factor $1-(\omega/\omega_{ci})^2$, which leads to a shift of the singularity $A = 0$: it occurs at $\omega = k_\parallel c_A(1+k_\parallel^2 c_A^2/\omega_{ci}^2)^{-1/2}$ instead of $\omega = k_\parallel c_A$. The "curvature" coefficient G (APPERT et al., 1982 a and b) is supplemented by the first term in the expression (8). Since the second term in (8) can be either negative or positive the finite frequency corrections can either decrease or increase the value of G. As shown in our previous work (APPERT et al., 1982 a) this coefficient plays a very important role in determining the rate of r.f. energy absorption and the position of an optimal resonance surface. Moreover, it gives rise to the existence of global eigenmodes of the Alfvén wave (APPERT et al., 1982 b and c). Thus, depending on the sign of $k_\parallel$, the finite frequency corrections may be expected either to enhance or to reduce the absorption rate, to shift the optimal resonance surface and to increase or to decrease the distance of the eigenfrequencies of the Alfvén global eigenmodes from the lower edge of the Alfvén continuum.

We now assume that the plasma oscillations are excited by an idealized antenna, consisting of a sheet current of given frequency and single helicity, which is located at a radius r_A in the vacuum region between the plasma column and a perfectly conducting wall of radius r_W:

$$\vec{J}_A = J_0 \left[k\hat{\theta} - (m/r_A)\hat{z} \right] \delta(r - r_A) \times \cos(\omega t) \cos(m\theta + kz) \, . \tag{9}$$

The resulting boundary-value problem can then be solved using the Maxwell equations in the vacuum and the equations (5) and (6) in the plasma requiring that $E_\perp$ and $B_\parallel$ be continuous at the plasma-vacuum interface. For the equilibrium quantities we choose profiles which are typical for Tokamak plasmas:

$$\rho = \rho(0)\left(1 - 0.95x^2\right) \quad , \quad B_{0z} = B_0 = const. ,$$

$$B_{0\theta} = B_0 \alpha x \left(3 - 3x^2 + x^4\right) , \tag{10}$$

where α is a small parameter, $x = r/a$ and a is the plasma radius. As for the antenna current we take $J_0 = acB_0/(8\pi)$. The equations are integrated numerically by means of the Runge-Kutta method with an appropriate choice of $\nu/\omega \ll 1$. Once the solution is found we calculate the absorbed power per unit length of the plasma according to

$$\mathcal{P} = -\left\langle \int \vec{J}_A \cdot \vec{E}\, dS \right\rangle = \frac{\pi}{2}\frac{\omega}{c} J_0 r_A \, \mathrm{Re}\, B_r \Big|_{r=r_A} \tag{11}$$

and/or

$$\mathcal{P} = \frac{ac}{8} \mathrm{Re}\left(E_\perp B_\parallel^*\right)\Big|_{r=a} \tag{12}$$

which are, of course, equivalent. Since the antenna current is held constant the absorbed power is equivalent to the real part of the antenna impedance.

3. RESULTS

We have performed different series of computations varying k, m, ω, and ω/ω_{ci} while the values of the other parameters were fixed: $\alpha = 0.1$, $r_A = 1.2a$ and $r_W = 1.5a$. The quantity ν was in the range $10^{-4} - 10^{-5}\ c_A(0)/a$.

3.1 Surface mode versus cavity modes

In the first study we tried to assess to what extent ω/ω_{ci} corrections affect the "competition" between the two schemes of resonant absorption mentioned in Section 1. For this purpose we followed the resonances of absorbed power in the ωk-space, corresponding to the excitation of the first and second radial eigenmodes, using different values of ω/ω_{ci} and a fixed value of m. Typical examples are shown in Figs. 1-3, where the absorbed power (a), the resonance width (b) and the radial position of the resonance surface (c) are plotted vs k. Here the resonance width $\Delta\omega$ is defined as the full width at half power. The quantity $\omega/\Delta\omega$ can be interpreted as the cavity Q. In general, we may note the following features. The power of the first mode is not much affected by the ω/ω_{ci} corrections whereas that of the second mode is drastically reduced. As expected the reduction is more pronounced in the case where $k_{\parallel} > 0$; this fact was already noticed by KARNEY et al. (1979). The finite frequency effects have a tendency to broaden the resonance widths. This is true especially for the second mode. The most important issue, however, are the positions of the resonance surface. For both the modes they are shifted towards the plasma boundary. Nevertheless, we may still conclude that it is somewhat easier to deposit the wave energy in the central part of the plasma via the excitation of the surface mode. For that reason we shall further discuss only this excitation scheme although the reader might take an interest in the advantageous loads of the second mode.

3.2 Absorption of the surface mode at the optimum

As can be seen from Figs. 1-3 the resonant absorption of the first mode is optimal at $|k| = 2.5$. In the next study we have investigated the ω/ω_{ci} effects on the dependence of the power on the position of the resonance surface, i.e. on the excitation frequency, at this optimum. The results are shown in Figs. 4-7, where the absorbed power is plotted vs the position of the resonance surface for different combinations of the signs of k and m. In the MHD limit (Fig. 4) we have, of course, only two combinations which are physically different. The ω/ω_{ci} corrections remove this "degeneracy" as we already noted in Section 2. It is easily seen that the MHD picture is radically changed even for a rather small value of ω/ω_{ci}, as demonstrated in Fig. 5. With increasing values of ω/ω_{ci} the deviation from the

MHD picture is more and more pronounced. We can roughly distinguish two cases. For $m > 0$ the peaks of absorbed power become narrower and they are pushed considerably towards the plasma boundary. For $m < 0$ the peaks become broader and finally they are spread nearly uniformly over the whole plasma cross-section. The fact that the m number controls the qualitative behaviour of the absorbed power for large values of ω/ω_{ci} can be understood by inspecting the equations (5), (6) and (8). The term proportional to $k_\parallel$ in (8) is negligible and the curvature coefficient is then controlled only by $k_\perp$ which, in turn, is dominated by m for small $B_{o\Theta}$.

It is evident that the mode having $m < 0$ and $k < 0$ exhibits the most spectacular modification due to the finite frequency effects. In particular, it seems to occur for rather small values of ω/ω_{ci}. In order to see this more in detail we varied the ratio ω/ω_{ci} by small steps in the range 0 - 0.1. In Fig. 8 we display the behaviour of the absorbed power vs the position of the resonance surface for different values of ω/ω_{ci}. We observe that the power has a distinct maximum at $\omega/\omega_{ci} = 0.075$. Thus, in addition to the other parameters (BALET et al., 1982) the ratio ω/ω_{ci} may even serve to optimize the resonant absorption of the surface mode.

3.3 Application to the TCA Tokamak

Recently power absorption experiments have been carried out on the TCA Tokamak using oscillating fields within the Alfvén wave range of frequencies (de CHAMBRIER et al., 1982 a and b). The general behaviour of the absorption was found to be in agreement with the MHD theory (APPERT et al., 1982 a, b and c). There are however two features which could not be interpreted satisfactorily. Firstly, the ω-spacing of resonance peaks, associated with the excitation of global eigenmodes of the Alfvén wave, is too large as compared to that obtained from the calculations. Secondly, the frequency dependence of the absorption within the Alfvén continuum is flatter than that found theoretically. We now wish to convey that these discrepancies may be explained by means of the present model which includes the ω/ω_{ci} corrections. Figure 9 shows the absorbed power vs the excitation frequency for different values of ω/ω_{ci}. The power was obtained as a sum of the powers delivered by four antennae with the ($m = 1$, $k = 0.6$), ($m = 1$, $k = -0.6$), ($m = -1$, $k = 0.6$), ($m = -1$, $k = -0.6$) helicities, each carrying the current $J_0/2$. It is clearly evidenced that the ω-spacing of the peaks increases and the "continuum" absorption curve flattens as the ω/ω_{ci} ratio increases. In order to avoid confusion we note that the last peaks correspond to the excitation of the cavity modes. The fact that the ω-spacing of the resonance peaks below the continuum may be modified by the finite frequency effects was already noticed by ROSS et al. (1982). Quantitative comparison between the present theory and recent experimental results from the TCA Tokamak will be the subject of a forthcoming publication (Pochelon, 1982 - private communication).

4. CONCLUSION

We have shown that the finite ω/ω_{ci} effects can dramatically modify the MHD picture of the resonant absorption of magnetoacoustic modes in Tokamak plasmas. In particular, they can change the magnitude of absorbed power, shift the position of the optimal resonance surface and broaden the resonance width. They can even be used to optimize the resonant absorption. Furthermore, they can modify the spectrum associated with global eigenmodes of the Alfvén wave. However, they do not change our previous conclusions concerning a certain superiority of the coupling scheme based on the excitation of the surface mode.

We have also demonstrated that the inclusion of ω/ω_{ci} corrections provides good qualitative agreement between MHD theory and recent experimental results.

Acknowledgements

The authors wish to acknowledge the fruitful discussions with D.W. Ross.

REFERENCES

APPERT K., BALET B. and VACLAVIK J. (1982a) Phys. Lett. 87A, 233.

APPERT K., GRUBER R., TROYON F., and VACLAVIK J. (1982b) 3rd Joint Varenna-Grenoble International Symposium on Heating in Toroidal Plasmas, Grenoble, Vol. I, p. 203.

APPERT K., GRUBER R., TROYON F. and VACLAVIK J. (1982c) Plasma Physics 24.

BALET B., APPERT K. and VACLAVIK J. (1982) Plasma Physics 24, 1005.

de CHAMBRIER A. et al. (1982a) Plasma Physics 24, 893.

de CHAMBRIER A. et al. (1982b) 3rd Joint Varenna-Grenoble International Symposium on Heating in Toroidal Plasmas, Grenoble, Vol. I, p. 161.

GROSSMANN W. and TATARONIS J. (1973) Z. Phys. 261, 217.

HASEGAWA A. and CHEN L. (1974) Phys. Rev. Lett. 32, 454.

KARNEY C.F.F., PERKINS F.W. and SUN Y.C. (1979) Phys. Rev. Letters 42, 1621.

References (cont'd)

ROSS D.W., CHEN G.L. and MAHAJAN S.M. (1982) Physics Fluids 25, 652.

STIX T.H. (1976) 3rd Symposium on Plasma Heating in Toroidal Devices, Varenna, September, p. 156.

STIX T.H. (1980) 2nd Joint Varenna-Grenoble International Symposium on Heating in Toroidal Plasmas, Como, Vol. II, 631.

FIGURE CAPTIONS

Fig. 1 Absorbed power (a), resonance width (b) and the position of resonance surface (c) vs the axial wavenumber for m = 1 and ω/ω_{ci} = 0. The normalizing power $P_N = a\ c_A(0)B_0^2/(4\pi)$.

Fig. 2 Absorbed power (a), resonance width (b) and the position of resonance surface (c) vs the axial wavenumber for m = 1 and ω/ω_{ci} = 0.3.

Fig. 3 Absorbed power (a), resonance width (b) and the position of resonance surface (c) vs the axial wavenumber for m = -1 and ω/ω_{ci} = 0.3.

Fig. 4 Absorbed power vs the position of resonance surface for ω/ω_{ci} = 0.

Fig. 5 Absorbed power vs the position of resonance surface for ω/ω_{ci} = 0.1.

Fig. 6 Absorbed power vs the position of resonance surface for ω/ω_{ci} = 0.3.

Fig. 7 Absorbed power vs the position of resonance surface for ω/ω_{ci} = 0.8.

Fig. 8 Absorbed power vs the position of resonance surface for different values of ω/ω_{ci}; $m = -1$, $ka = -2.5$.

Fig. 9 Absorbed power vs the excitation frequency for different values of ω/ω_{ci} in the case of a TCA antenna model.

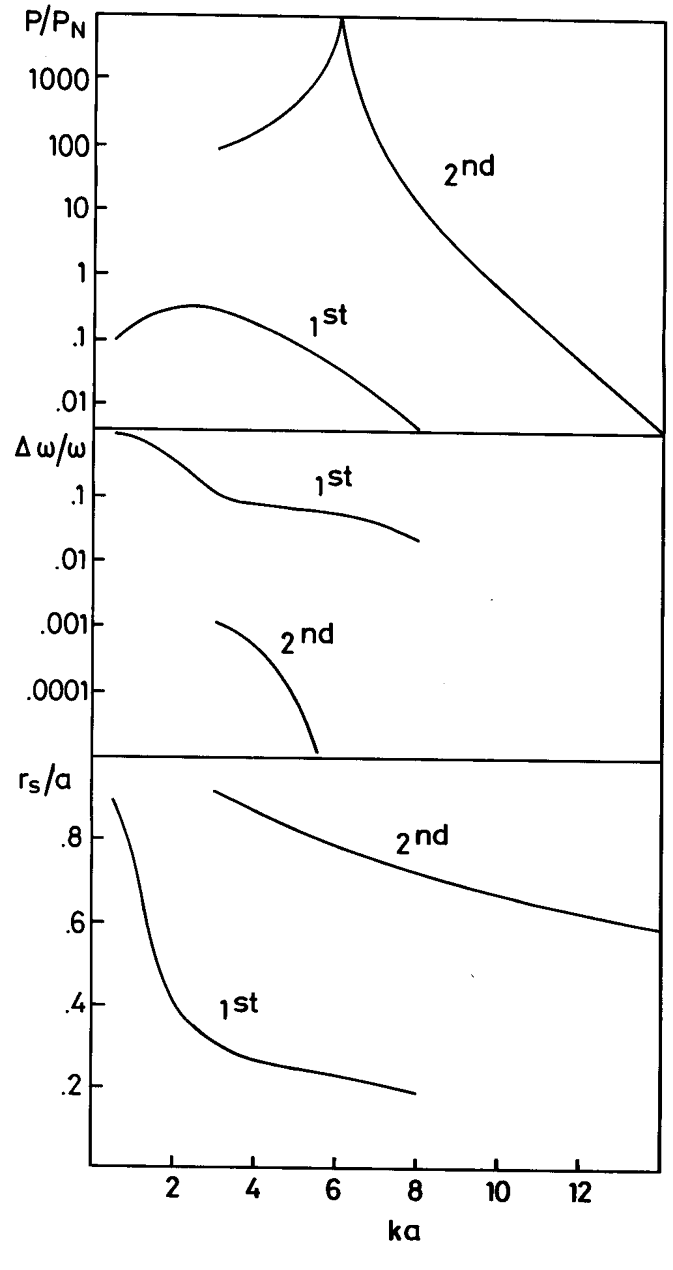

P/P_N
1000
100
10
1
.1
.01
2nd
1st
Δω/ω
.1
.01
.001
.0001
1st
2nd
r_s/a
.8
.6
.4
.2
2nd
1st
2
4
6
8
10
12
ka

FIG. 1

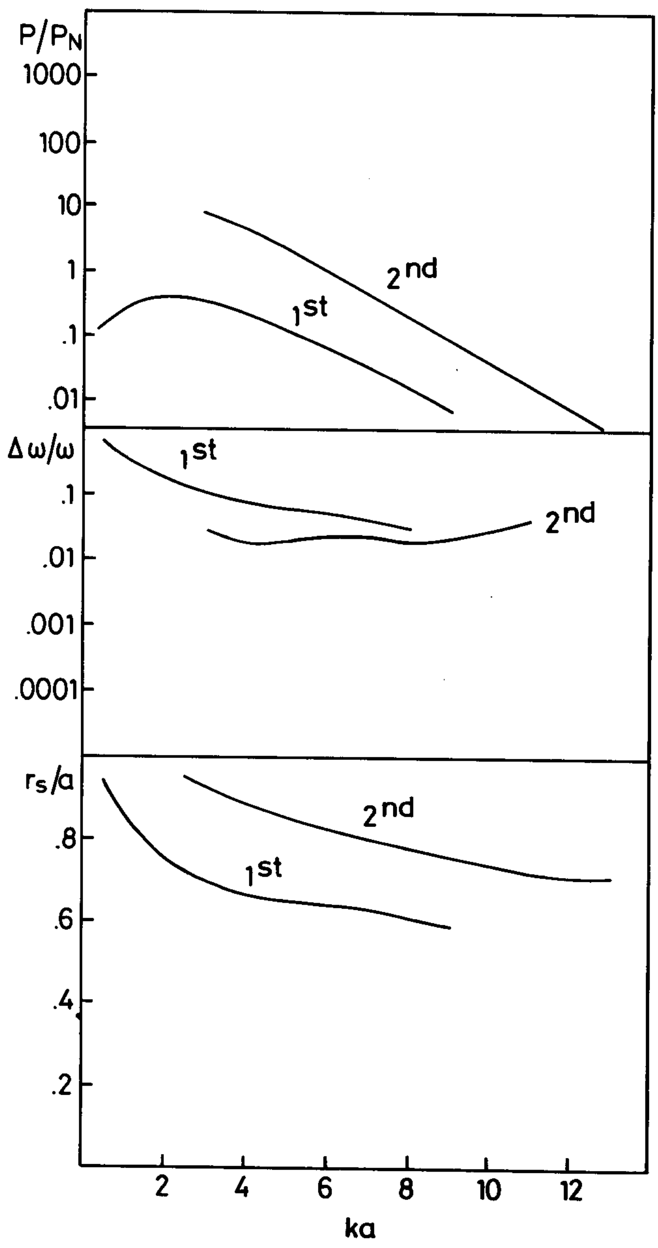
P/P_N
1000
100
10
1
.1
.01
2nd
1st
Δω/ω
.1
.01
.001
.0001
1st
2nd
r_s/a
.8
.6
.4
.2
2nd
1st
2
4
6
8
10
12
ka

FIG. 2

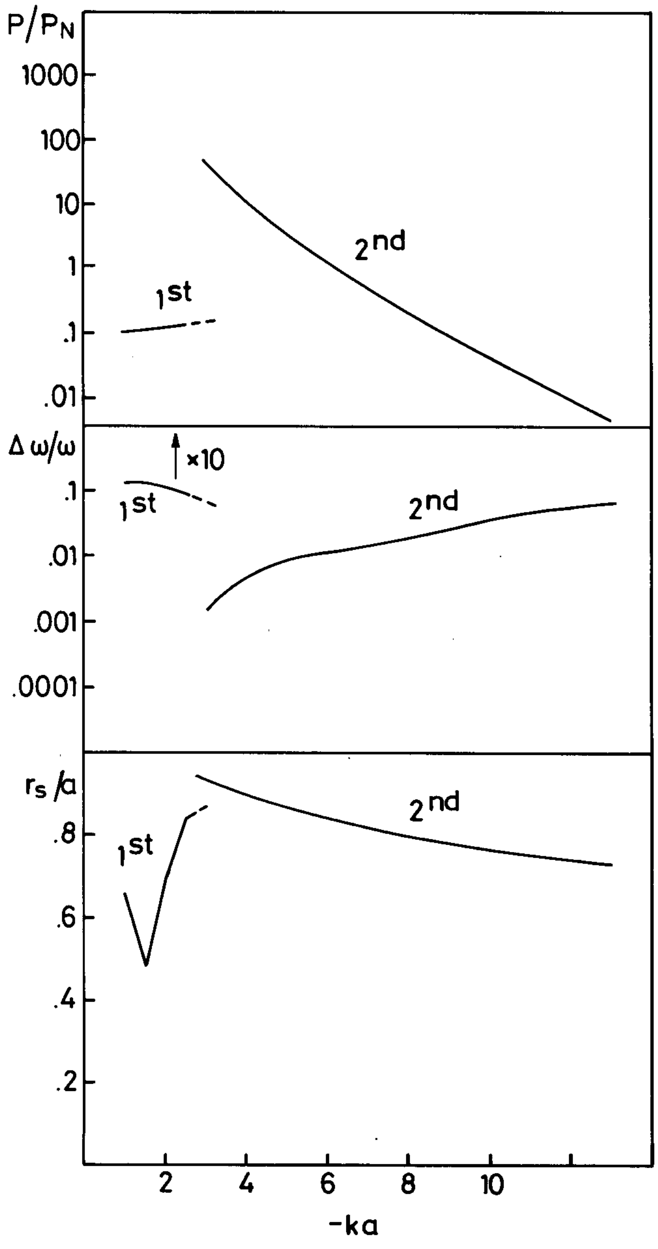
P/PN
1000
100
10
1
.1
.01
1st
2nd
Δω/ω
×10
.1
.01
.001
.0001
1st
2nd
rs/a
.8
.6
.4
.2
1st
2nd
2
4
6
8
10
-ka

FIG. 3

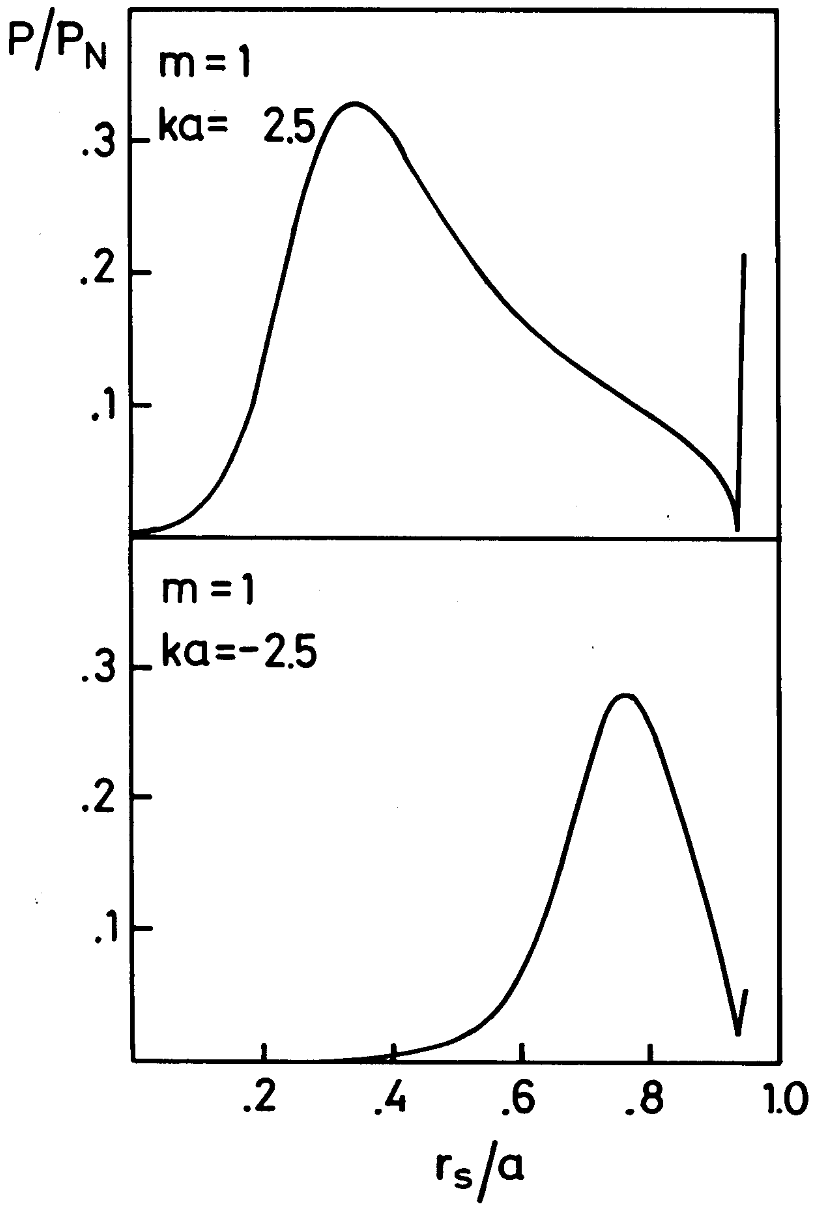

FIG. 4

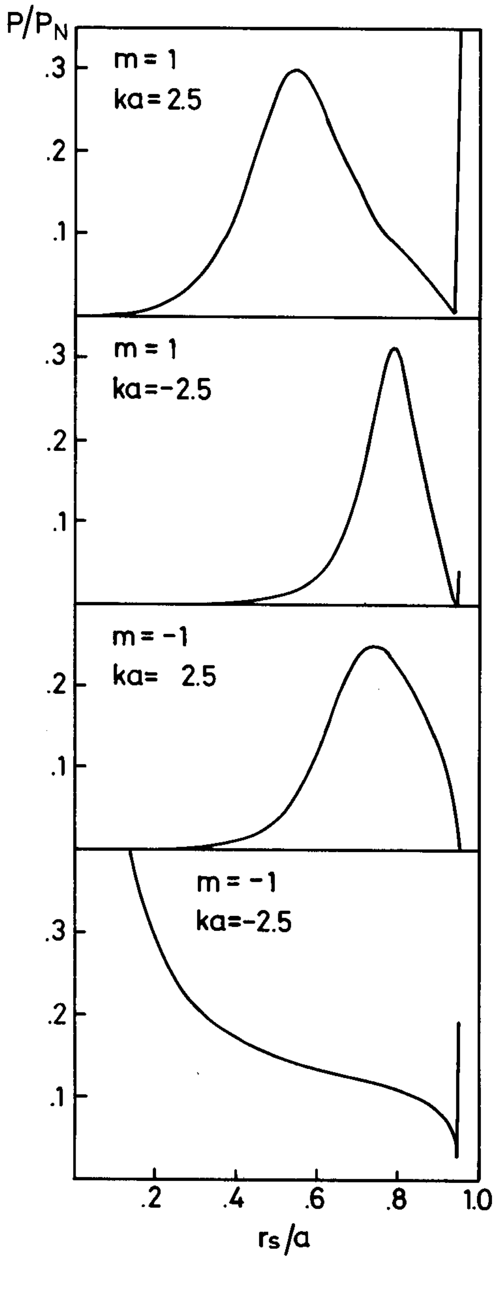

FIG. 5

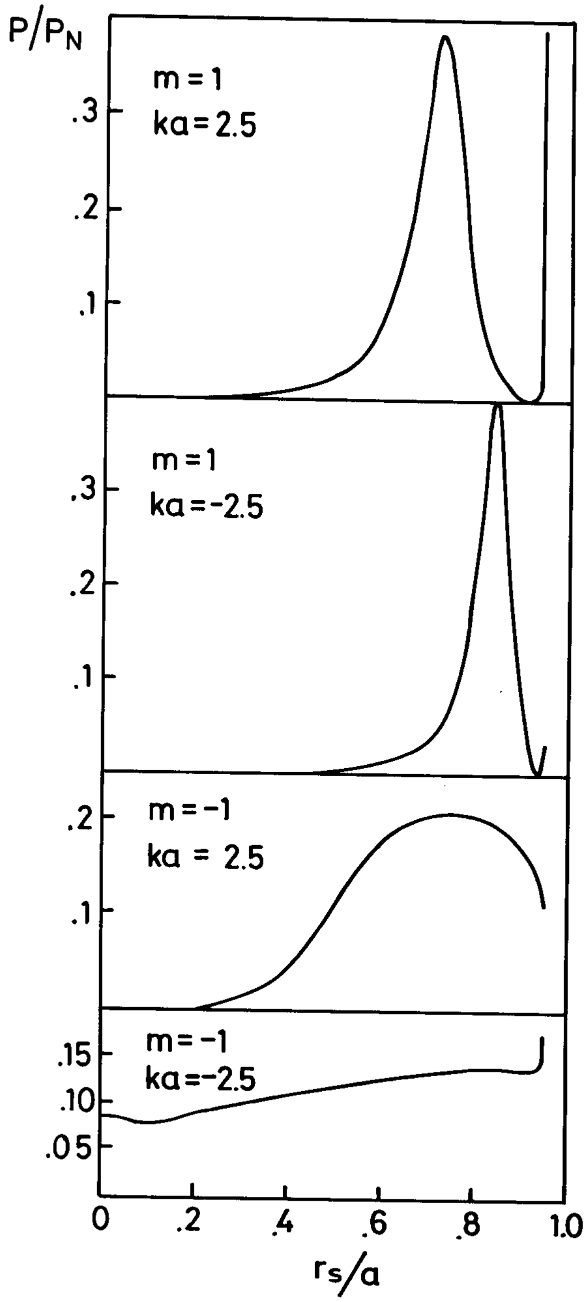
P/P_N
m = 1
ka = 2.5
.3
.2
.1
m = 1
ka = -2.5
.3
.2
.1
m = -1
ka = 2.5
.2
.1
m = -1
ka = -2.5
.15
.10
.05
0
.2
.4
.6
.8
1.0
r_s/a

FIG. 6

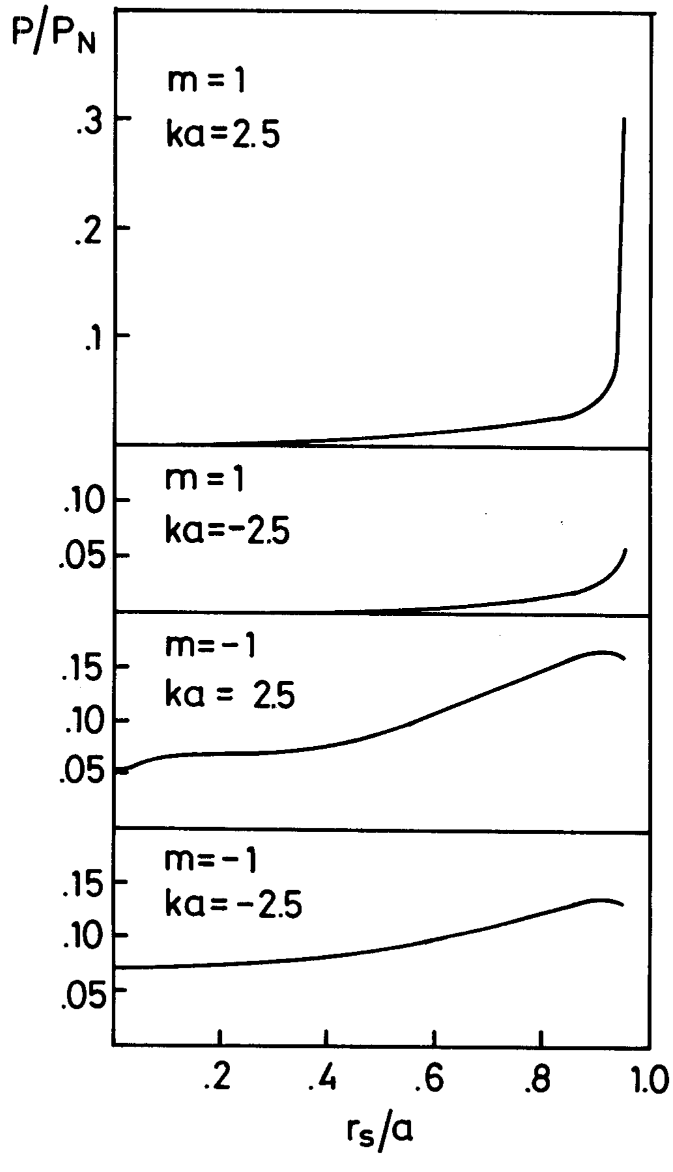
P/P_N
m = 1
ka=2.5
.3
.2
.1
m = 1
ka=-2.5
.10
.05
m=-1
ka = 2.5
.15
.10
.05
m=-1
ka=-2.5
.15
.10
.05
.2
.4
.6
.8
1.0
r_s/a

FIG. 7

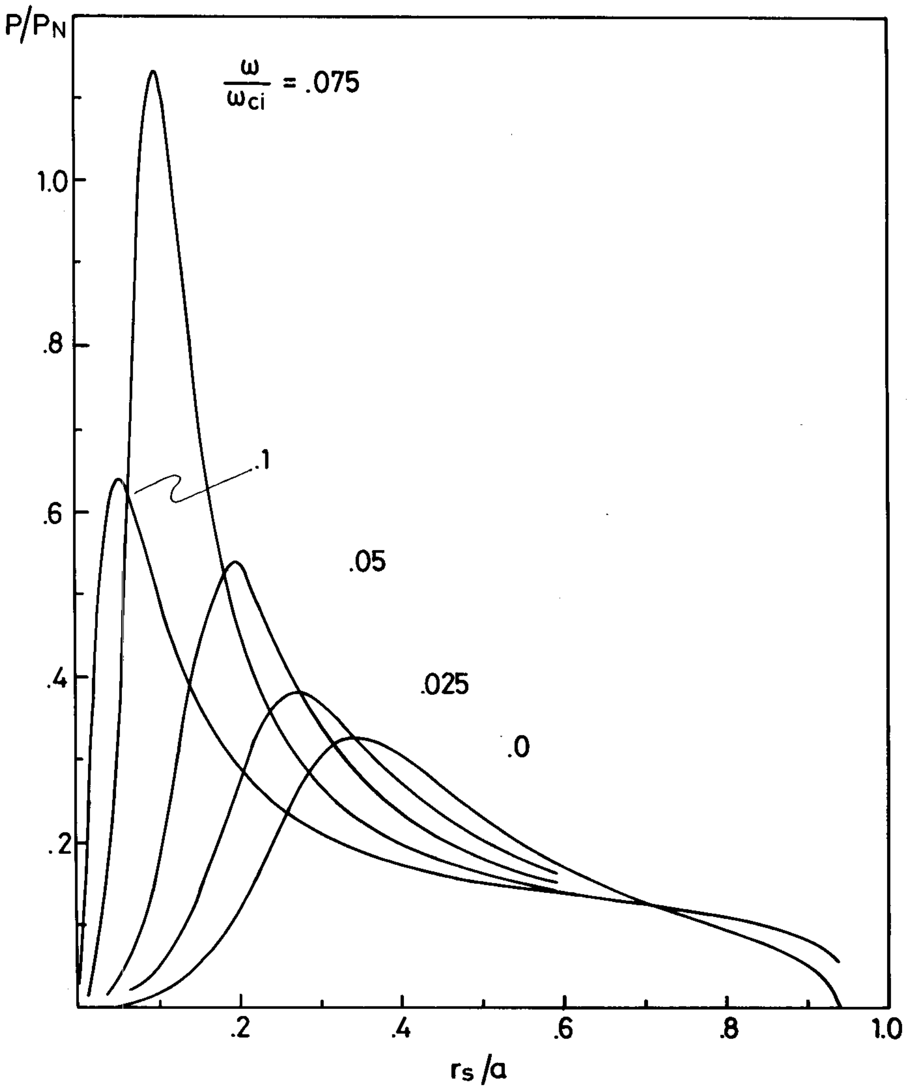

FIG. 8

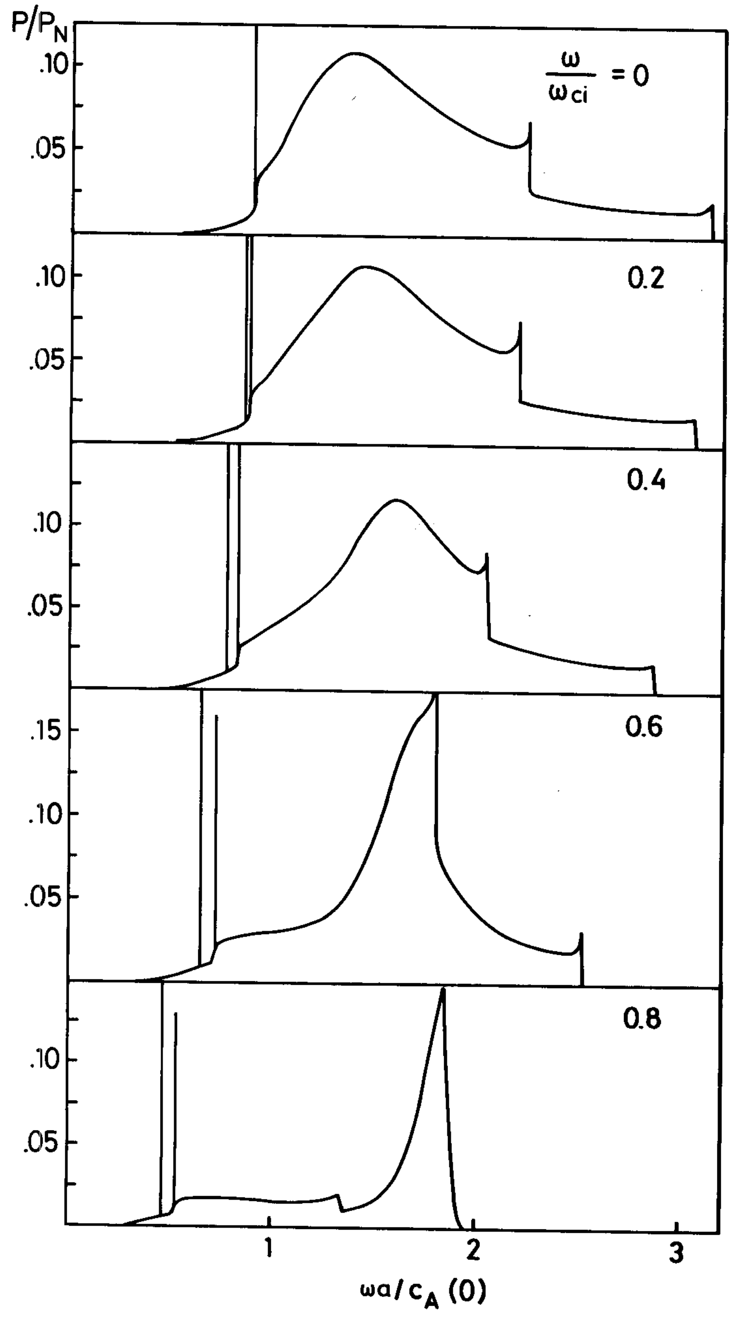

FIG. 9